Block Copolymer Directed One-Pot Simple Synthesis of $L1_0$-Phase FePt Nanoparticles inside Ordered Mesoporous Aluminosilicate/Carbon Composites

Eunae Kang,[†] Hyunok Jung,[§] Je-Geun Park,[§] Seungchul Kwon,[†] Jongmin Shim,[†] Hiroaki Sai,[⊥] Ulich Wiesner,[⊥] Jin Kon Kim,[†,*] and Jinwoo Lee[†,‡,*]

[†]Department of Chemical Engineering, Pohang University of Science and Technology, San 31, Hyo-ja dong, Pohang, 790-784, Korea, [‡] School of Environmental Science and Engineering, Pohang University of Science and Technology, San 31, Hyo-ja dong, Pohang, 790-784, Korea, [§] Department of Physics and Astronomy, Center for Strongly Correlated Materials Research, Seoul National University, Seoul 151-747, Korea, and [⊥] Department of Materials Science and Engineering, Cornell University, Ithaca, NY 14853, United States

ABSTRACT A "one-pot" synthetic method was developed to produce $L1_0$-phase FePt nanoparticles in ordered mesostructured aluminosilicate/carbon composites using polyisoprene-*block*-poly(ethylene oxide) (PI-*b*-PEO) as a structure-directing agent. PI-*b*-PEO block copolymers with aluminosilicate sols are self-assembled with a hydrophobic iron precursor (dimethylaminomethylferrocene) and a hydrophobic platinum precursor (dimethyl(1,5-cyclooctadiene)platinum(II)) to obtain mesostructured composites. The as-synthesized material was heat-treated to 800 °C under an Ar/H_2 mixture (5% v/v), resulting in the formation of fct FePt nanocrystals encapsulated in ordered mesopores. By changing the quantities of the Fe and Pt precursors in the composite materials, the average particle size of the resulting fct FePt, estimated using the Debye−Scherer equation with X-ray diffraction patterns, can be easily controlled to be 2.6−10.4 nm. Using this simple synthetic method, we can extend the size of directly synthesized fct FePt up to ~10 nm, which cannot be achieved directly in the colloidal synthetic method. All fct FePt nanoparticles show hysteresis behavior at room temperature, which indicates that ferromagnetic particles are obtained inside mesostructued channels. Well-isolated, ~10 nm fct FePt have a coercivity of 1100 Oe at 300 K. This coercivity value is higher than values of fct FePt nanoparticles synthesized through the tedious hard template method by employing SBA-15 as a host material. The coercivity value for FePt-1 (2.6 nm) at 5 K is as high as 11 900 Oe, which is one of the largest values reported for FePt nanoparticles, or any other magnetic nanoparticles. The fct FePt nanoparticles also showed exchange-bias behavior.

KEYWORDS: block copolymer · $L1_0$-phase FePt · aluminosilicate · self-assembly · mesoporous structure · magnetic properties

Ordered assemblies of hard magnetic FePt nanocrystals are of great importance in magnetic data storage media.[1] Face-centered tetragonal (fct) FePt is known to exhibit large uniaxial magnetocrystalline anisotropy and high coercivity, properties that make it well suited for use in magnetic storage media.[2] Preparation of size-controlled fct FePt nanocrystals is a prerequisite for the fabrication of ordered assemblies of hard magnetic FePt. Chemical routes have frequently been employed to synthesize monodisperse FePt nanocrystals.[3−8] Chemical colloidal synthesis at low temperatures (~300 °C) typically produces superparamagnetic face-centered cubic (fcc) FePt nanocrystals. Chemically synthesized FePt nanocrystals have to be heat-treated at 550 °C or more to obtain fct-phase (the so-called $L1_0$ structure) FePt.[9,10] However, the surfactants coating the particles get easily decomposed at these temperatures, leading to the agglomeration of monodisperse FePt nanoparticles. The resulting undefined and sintered structure is not suitable for use in high-density recording media. Avoiding particle coalescence is one of the most challenging problems in the production of materials from FePt nanoparticles for high-density magnetic data storage. There is, therefore, a need to develop a new method for the production of fct $L1_0$-phase nanocrystals without agglomeration during the heat treatment at high temperatures (>550 °C). Several methods have been developed to prevent nanocrystals from agglomerating during the conversion to fct materials. The introduction of a third metal, such as Ag, lowered the transition temperature to around 400 °C, but the ternary nanoparticles coated with surfactants might be still agglomerated after removal of surfactants during heat treatment at 400 °C.[11] Agglomeration could be prevented by the synthesis of a silicate or MgO/Fe_3O_4 multishells on as-synthesized cubic FePt nanoparticles.[12−14] However, preformed fcc FePt nanoparticles

* Address correspondence to jkkim@postech.ac.kr, jinwoo03@postech.ac.kr.

Received for review September 18, 2010 and accepted January 5, 2011.

Published online January 12, 2011
10.1021/nn102451y

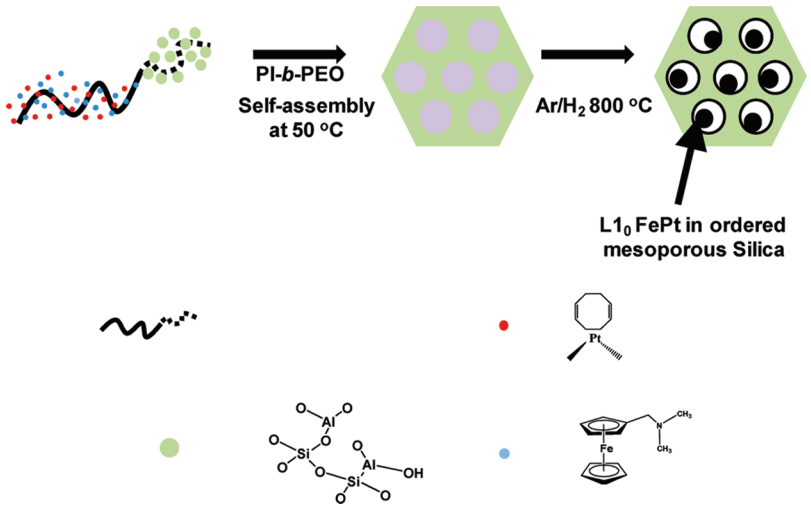

Scheme 1. Schematic representation of the preparation of fct FePt nanocrystals inside ordered mesostructured aluminosilicate/carbon.

must be synthesized through a colloidal method, and a delicate silicate or MgO/Fe_3O_4 multishell coating process and further heating at high temperature (~800 °C) are required to obtain fct FePt. Mesoporous silica (SBA-15) was employed as a hard exotemplate to prevent agglomeration during formation of fct FePt.[15] Although SBA-15 mesoporous silica can be used as a host material to prevent the agglomeration of FePt particles during the conversion of fcc FePt to fct FePt at high temperature, the long and complicated synthetic procedure would limit the practical applications of this method. Namely, the synthetic process involved preparation of an ordered mesoporous silica, backfilling with $Fe(acac)_3$ and $Pt(acac)_2$ by multiple impregnations (five to six filtration cycles), and heat treatment at high temperatures (800 °C) to convert the precursors to fct FePt. Furthermore, powder-type mesoporous silica (SBA-15) used as a hard exotemplate cannot be applied to fabricate FePt dot arrays on a desired substrate for future ultra-high-density data storage media.

Another important issue on the FePt nanoparticles is the synthesis of large-sized fct FePt nanoparticles. For practical applications of fct FePt nanoparticles, it is required that one synthesizes large-sized FePt nanoparticles (~10 nm) to achieve high coercivity (H_c) and remanance to the saturation magnetization ratio M_r/M_s.[16,17] However, colloidal synthetic methods typically yield fcc FePt particles with sizes of 4−6 nm. To produce large fct FePt nanocrystals, a Pt/Fe_2O_3 core/shell nanoparticle with a 10 nm core and a 3.5 nm shell was synthesized and then heat-treated to achieve conversion to fct FePt.[16] However, because of the very high coercivity values of fct FePt structures (~5000 Oe at 300 K) at 300 K and sharp X-ray diffraction (XRD) patterns of heat-treated films, we cannot exclude the possibility of surfactant decomposition and sintering of the resulting fct FePt particles into larger crystals after heat treatment at 550 °C. In this context, it is challenging to develop a simple and straightforward synthetic method for direct production of large-sized (~10 nm) fct FePt nanocrystals.

In this paper, we present a new, simple method for the production of $L1_0$-phase FePt nanoparticles with a controllable average size. A "one-pot" synthetic method was developed for producing $L1_0$-phase FePt nanoparticles in ordered mesostructured aluminosilicate/carbon composites using polyisoprene-*block*-poly(ethylene oxide) (PI-*b*-PEO) copolymer as a structure-directing agent.[18] For this "one-pot" synthesis of $L1_0$-phase FePt nanoparticles, it is required that one selectively patterns hydrophobic metal precursors in the hydrophobic part of the block copolymer. If commercially available amphiphilic block copolymers, such as pluronic block copolymers [poly(ethylene oxide)-*block*-poly(propylene oxide)-*block*-poly(ethylene oxide) copolymer $(EO)_x-(PO)_y-(EO)_x$], are employed, hydrophobic metal precursors will not be selectively incorporated into the hydrophobic phase (PPO) due to an insufficient difference in hydrophilicity and hydrophobicity.[19] To provide a sufficient difference in hydrophilicity and hydrophobicity for the selective incorporation of hydrophobic metal precursors, PI-*b*-PEO was synthesized through anionic polymerization and used as a structure-directing agent. By the current fabrication method, ~10 nm sized large fct FePt nanoparticles can be directly synthesized inside mesostructured silica/carbon composites, and this current "one-pot" synthetic method is potentially applicable to fabricate fct FePt nanodot film-type arrays by simple spin-coating or dip-coating of the prepared solutions.

RESULT AND DISCUSSION

Scheme 1 shows a synthetic route for the synthesis of fct FePt nanoparticles, with a controllable average particle size, inside mesostructured silica/carbon composites. PI-*b*-PEO block copolymers with aluminosilicate

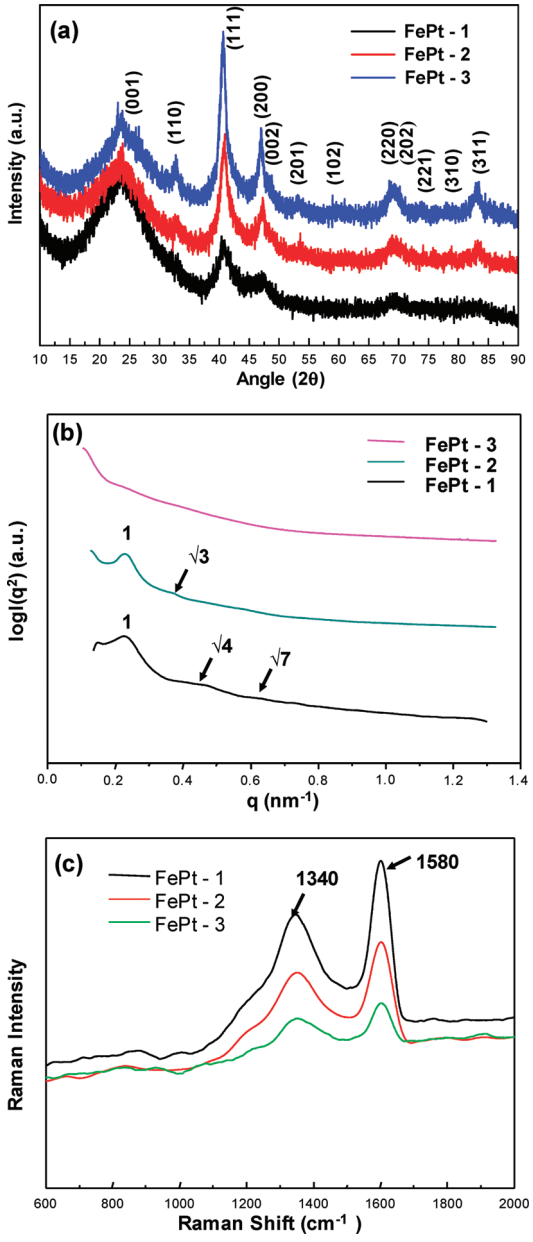

Figure 1. (a) XRD patterns, (b) SAXS traces, and (c) Raman spectroscopy data of FePt-1, FePt-2, and FePt-3.

sols are mixed with a hydrophobic iron precursor (dimethylaminomethyl-ferrocene) and a hydrophobic platinum precursor (dimethyl(1,5-cyclooctadiene)platinum(II)). Bulk films were cast by evaporation of the solvent in air on a hot plate at 50 °C and then at 130 °C in a vacuum oven for 1 h. The as-synthesized material was heat-treated to 800 °C, using a 1 °C min^{-1} ramp, under an Ar/H_2 mixture (5% v/v) and held at that temperature for at least 2 h, resulting in the formation of fct FePt nanocrystals encapsulated in ordered mesopores. By changing the quantities of the Fe and Pt precursors in the solution relative to the amount of aluminosilicate sol, the average particle size of the resulting fct FePt, estimated using the Debye−Scherer equation, can be easily controlled to be 2.6−10.4 nm. The FePt loading levels used in the ordered mesoporous carbon/silica composite relative to the amount of aluminosilicate remaining after high-temperature treatment (~800 °C) were 5 wt % (FePt-1), 10 wt % (FePt-2), and 15 wt % (FePt-3). Mesostructured aluminosilicates assembled using PI-*b*-PEO are known to be stable at high temperatures (as high as 800 °C) because of their thick walls (>10 nm), which prevent aggregation of FePt nanoparticles during conversion to fct FePt.[20]

In our method, all the metal precursors were added to a solution of the PI-*b*-PEO block copolymer and aluminosilicate sol, thereby eliminating the tedious process of preparing ordered mesoporous silica and then backfilling with metal precursors, which is required when a mesoporous silica was used as a hard exotemplate.[15]

The synthesized FePt nanoparticles were characterized by scanning electron microscopy (SEM), transmission electron microscopy (TEM), X-ray diffraction (XRD), small-angle X-ray scattering (SAXS), Raman spectroscopy, and SQUID magnetometer measurements.

The XRD patterns show that all the FePt nanoparticles have typical fct structures (Figure 1). The changes in the breadths of the (111) peaks indicate that higher precursor loadings generated larger fct FePt particles. The formation of the fct FePt phase was shown by the appearance of (110) peaks in the XRD patterns of all the FePt samples. The average crystallite size was calculated using the Debye−Scherer equation.[21] The average particle sizes of FePt-1, FePt-2, and FePt-3 were 2.6, 6.8, and 10.4 nm, respectively. Using this simple synthetic method, we can extend the size of directly synthesized fct FePt up to ~10 nm, which cannot be achieved directly in the colloidal synthetic method.

The volume of the unit cell of pure fct FePt is expected to be 55.1 $Å^3$ (JCDPS: 43-1359). The calculated value of the volume unit cell of fct FePt-3 with size of 10.4 nm was 55.6 $Å^3$, implying that the crystal structure of fct FePt-3 is almost similar to that of pure fct FePt.

It has been reported that the poly(isoprene), which contains two sp^2 carbons per monomer unit, was converted to carbon materials after high-temperature treatment under an inert atmosphere when PI-*b*-PEO block copolymers were used as structure-directing agents for mesostructured materials.[22,23] The presence of carbon in the FePt samples was proven by Raman spectroscopy (Figure 1c). In all the FePt samples, bands attributable to graphitic carbon and disordered carbon appear at around 1580 and 1340 cm^{-1}.

The ordered mesostructures containing FePt were characterized by SAXS (Figure 1b). FePt-1 and FePt-2 exhibit the typical SAXS patterns for hexagonally ordered structures. The arrows in Figure 1b indicate the angular positions of $3^{1/2}$ and $4^{1/2}$ for the first-order maximum (d_{100} ~ 27.8 nm for FePt-1, d_{100} ~ 28.5 nm for FePt-2), as expected for a hexagonally ordered structure. The d_{100} values obtained by SAXS were

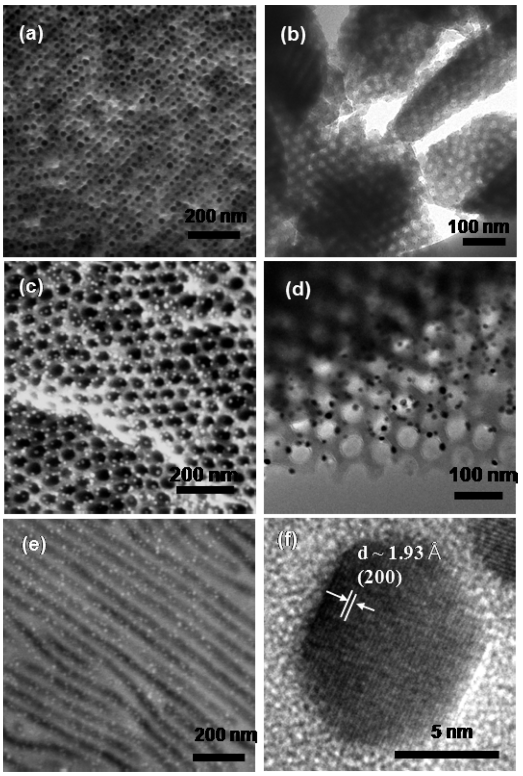

Figure 2. SEM images of (a) FePt-1 and (c, e) FePt-3. TEM images of (b) FePt-1 and (d) FePt-3. (f) HRTEM image of FePt-3.

consistent with d_{100} values obtained from TEM and SEM images (Figure 2 and Figures S1 and S2 in the Supporting Information).

After heat treatment at 800 °C, the ordered structures of the as-synthesized composites were preserved, and the SAXS patterns showing the degree of long-range ordering indicate thermal stability of the aluminosilicates synthesized by the PI-*b*-PEO structure-directing agents. Interestingly, in the case of FePt-3, the d_{100} spacing observed by TEM (Figure 2d) was 64 nm, so, because of experimental limitations, the first-order maximum peak was not detected. The d_{100} spacing of the mesostructure in the FePt-3 sample was calculated using the second-order peak (angular position of $3^{1/2}$) to be 58 nm.

In this work, hydrophobic metal precursors were used as metal sources and pore expanders. The sudden increase in $d_{spacing}$ in FePt-3 indicates that there is a threshold point where the hydrophobic metal precursors effectively begin to act as pore expanders.[24]

TEM and SEM images of FePt-1, FePt-2, and FePt-3 (Figure 2 and Figures S1 and S2 in the Supporting Information) show the highly ordered structure of the mesoporous aluminosilicate/carbon composites. These images also show that FePt nanoparticles—detected as black spots in TEM images and white spots in SEM images—are located inside the ordered mesopores. As observed in the XRD pattern of FePt-1, small (~2.6 nm) FePt particles are homogeneously dispersed inside the pores. In the case of FePt-3, FePt nanoparticles of approximately 10 nm are detected in the SEM and TEM images, consistent with the XRD pattern of FePt-3. The high-resolution transmission electron micrograph (HRTEM) presented in Figure 2f shows the highly crystalline structure of FePt-3 nanoparticles and d_{200} spacings of the fct FePt structure. The elemental composition of FePt-3 was $Fe_{42}Pt_{58}$, which was determined by using energy-dispersive X-ray spectroscopic (EDX) analysis of individual nanoparticles in HRTEM by choosing individual nanoparticles.

To show that PI-*b*-PEOs are very effective to synthesize well-dispersed fct FePt nanocrystals inside the channels of mesostructured materials, we used a commercially available block copolymer, F127 ($(EO)_{106}$-$(PO)_{70}(EO)_{106}$) as a structure-directing agent for the assembly with a hydrophobic iron precursor (dimethylaminomethyl-ferrocene), a hydrophobic platinum precursor (dimethyl(1,5-cyclooctadiene)platinum(II)), and aluminosilicate nanoparticles. In this situation, the metal precursors are expected to be selectively incorporated in the hydrophobic PPO block, whereas aluminosilicate nanoparticles are expected to be incorporated in the hydrophilic PEO block. The as-synthesized composite made with F127 was heat-treated to 800 °C to obtain FePt particles in the same way for the PI-*b*-PEO/metal precursors/aluminosilicate composite. Very interestingly, as shown in a TEM image (Figure S3 in the Supporting Information), most of FePt particles were greatly agglomerated and the particle size was much larger than the expected channel size of mesoporous silica templated by F127 (typically 4−6 nm).[25] This is because PPO in F127 does not provide sufficient hydrophobicity for the complete incorporation of hydrophobic metal precursors. Thus, some of the metal precursors exist outside of the pores, resulting in formation of an agglomeration of FePt particles during heat treatment at 800 °C. This result shows that, to confine fct FePt nanoparticles inside the channels of mesostructured materials, the difference between hydrophobicity and hydrophilicity in an amphiphilic block copolymer[19] should be large enough to contain all of the hydrophobic metal precursors into the hydrophobic block.

One of the determining factors for the block copolymer phase behavior is the Flory−Huggins segment−segment interaction parameter, χ. When the χ value is high, the unlike segments in block copolymers tend to segregate into ordered periodic structures. The $\chi_{PEO\text{-}PI}$ value ($\chi_{PEO\text{-}PI} = 65/T + 0.125$)[26] is larger than the $\chi_{PEO\text{-}PPO}$ value ($\chi_{PEO\text{-}PI} = 20.2/T + 0.0221$)[27] at the same temperature. Higher $\chi_{PEO\text{-}PI}$ than $\chi_{PEO\text{-}PPO}$ corroborates that PI-*b*-PEOs are very effective for selective incorporation of hydrophobic metal precursors because PI chains strongly segregate from PEO chains.

To study the limitation of precursor loading, the metal loading was increased to 20 wt % relative to the amount of aluminosilicates. The as-synthesized

composite material was heat-treated to 800 °C under Ar/H_2 (5 wt %) and kept at this temperature for 2 h. In this case, all the metal precursors might not be incorporated into mesostructures and part of the metal precursors might be self-aggregated into large-sized particles. The SEM image (Figure S4 in the Supporting Information) of the resulting heat-treated sample shows that mesostructures were formed around bright and large-sized particles. From the high atomic number of Fe and Pt compared with that of aluminosilicate/carbon, it is inferred that large-sized core particles are FePt. When the loading of FePt was increased to 20 wt %, part of the hydrophobic Fe and Pt precursors are assembled into mesostructures with PI-*b*-PEO and aluminosilictes. The remaining hydrophobic metal precursors might be expelled from the mesostructures during self-assembly, forming large-sized FePt nanoparticles around which mesostructured aluminosilicates grew. A similar phenomenon was reported by Warren *et al.*[28] When mesostructured materials are formed *via* self-assembly of PI-*b*-PEO with aluminosilicate nanoparticles, nanoparticles larger than a critical size were segregated out, forming a large-sized silica aggregate core structure around which an ordered mesostructure grew.

To check whether the particle size of fct FePt can be increased by using the higher-molecular-weight block copolymer, PI-*b*-PEO with an M_n of 104 000 g mol^{-1} (PEO content = 8.65 wt %, polydispersity index = 1.05) was used as a structure-directing agent to make mesostructured composite materials. The resulting composite was also heat-treated to 800 °C under Ar/H_2 (5 wt %) and kept at this temperature for 2 h to make fct FePt nanoparticles. Hydrophibic Fe and Pt precursors corresponding to 15 wt % of FePt relative to aluminosilicate (the loading of Fe and Pt precursors in FePt-3) were added during the mesostructure formation. As shown in Figure S5 (Supporting Information), the average size of the nanoparticles was 12.9 nm, somewhat larger than that of FePt-3 (10.0 nm). This result indicates that a change in dimension of structure-directing block copolymers is one of the factors that controls the particle size of fct FePt. In the case when we employ PI-*b*-PEO with an M_n of 30 000 g mol^{-1} as a structure-directing agent, the increase of metal loading from 5 to 15 wt % increased the particle size from 2.7 to 10 nm. However, when the molecular weight of block copolymers was changed from 30 000 to 104 000 g mol^{-1}, the particle size was only increased from 10 to 12.9 nm. With this result, we can conclude that the increased loading of metal precursors is more effective in increasing the particle size. However, further research is needed for a fine control of the fct FePt particle size inside ordered mesoporous aluminosilicat/carbon composites.

To understand the magnetic properties, we measured the magnetizations of FePt-1, FePt-2, and FePt-3 using a SQUID magnetometer after field-cooling (FC), and with zero-field-cooling (ZFC), at 100 Oe (Figure S7 in the Supporting Information). Although the particle sizes are relatively small, our data did not show clear signs of blocking behavior in the magnetization data, probably because of the large magnetic anisotropy constant and broad size distribution, as shown in Figure S6 (Supporting Information). We note that the smallest FePt nanoparticles, that is, FePt-1 with a size of 2.6 nm, show hysteresis behavior at room temperature. The observed particle distribution is broad, so this behavior probably results from the presence of some particles significantly larger than the mean value. On cooling, the coercivity value (H_c) increases significantly (Figure 3). It should be noted that our coercivity values for the three samples are much higher than values reported in the literature.[15] For example, the largest particle, FePt-3, with a particle size of 10.4 nm, has a coercivity of 1100 Oe at 300 K, which is ~18 times larger than the value of 60 Oe for FePt-O-1050 with a size of 10.8 nm, reported in ref 15. It is of particular interest that the coercivity of FePt-1 at 5 K is as high as 11 900 Oe, which is one of the largest values reported for FePt nanoparticles, or for any other magnetic nanoparticles. The other notable feature in our data is that all our samples clearly show signs of exchange-bias phenomena. As shown in Figure 4, the magnetization data are shifted in the negative field direction. This exchange-bias behavior is much stronger for the larger particles. We can define the exchange-bias field as $H_E = (H_{CL} - H_{CR})/2$, where H_{CL} and H_{CR} are the left- and right-hand-side coercivity values, respectively. An average coercive field is defined as $H_C = (H_{CL} + H_{CR})/2$. As summarized in Table 1, all the samples have sizable exchange-bias field (H_E) values at 5 K, and in the case of FePt-3, H_E is nonzero even at room temperature.

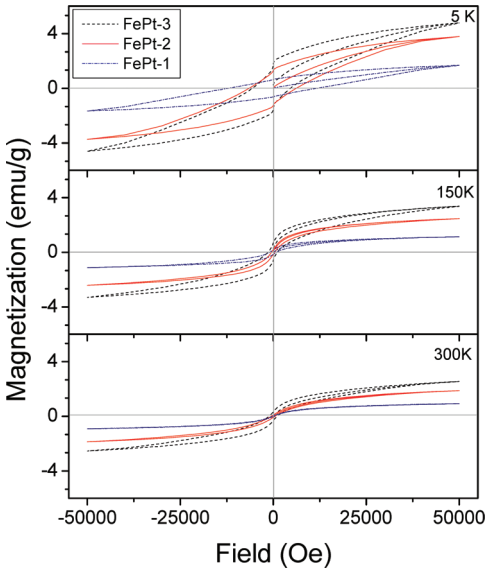

Figure 3. Hysteresis curves of FePt-1 (blue dashed-dotted line), FePt-2 (red solid line), and FePt-3 (black dashed line) measured at 5, 150, and 300 K.

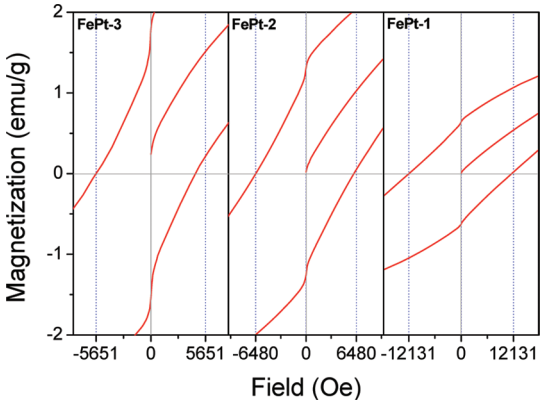

Figure 4. Enlarged plot of magnetization data for the low-field region showing asymmetric shift of the data. All the data were obtained at 5 K. The vertical dashed lines (blue) indicate the left- and right-hand coercive field values. Note the significant shift in the magnetization data for FePt-3 nanoparticles.

TABLE 1. Average Coercivity Field (H_c) and Exchange Bias (H_{ex}) of FePt-1, FePt-2, and FePt-3 at 5, 150, and 300 K

	average H_c			exchange bias H_{ex}		
	5 K	150 K	300 K	5 K	150 K	300 K
FePt-1	11 900	900	200	−200	−30	0
FePt-2	6300	400	500	−150	−60	0
FePt-3	5100	1300	1100	−530	−170	−30

The key observations regarding the magnetic properties, in particular, the exchange-bias phenomenon, need to be explained. Exchange-bias behavior, first reported for Co particles,[29] occurs when ferromagnetic components of the magnetic system are pinned by antiferromagnetic components. This has been well established for magnetic thin films.[30] However, it has been observed less often in magnetic nanoparticles, despite the original discovery being made for Co particles. However, there are now a few reports of exchange-bias behavior for magnetic nanoparticles.[31] Generally, magnetic nanoparticles have a core−shell structure, which leads to exchange-bias behavior. At present, we think that the chemical compositions of surfaces of fct FePt nanoparticles synthesized in this study might be slightly different than those of their core. This has been observed in the synthesis of magnetite/maghemite nanoparticles.[32] This variation in composition can lead to a different magnetic structure, which would then give rise to the observed exchange-bias behavior.

This approach can be extended to fct FePt nanocrystals confined in mesostructured aluminosilicate with other morphologies. With increasing aluminosilicate contents, the mesostructured morphology can be changed from hexagonal mesostructures to body-centered cubic (bcc) mesostructures. If FePt nanocrystals are confined in the pores of bcc mesostructures, FePt nanocrystals in one cubic pore could be isolated from FePt nanocrystals in other cubic pores. Resultantly, interparticle dipole−dipole interaction in magnetic nanoparticles could be controlled by employing mesostructured aluminosilicate with body-centered cubic morphologies.[33]

CONCLUSIONS

We have shown that fct FePt nanoparticles with a controllable average size could be synthesized inside ordered mesoporous silica/carbon materials by a one-pot synthetic method using PI-*b*-PEOs. The choice of PI-*b*-PEO is very unique because it gives a sufficient difference in hydrophilic and hydrophobic properties. With another amphiphic block copolymer with an insufficient difference, which is the case of Pluronic copolymer, the nanoparticles could not be confined into the hydrophobic block. After high-temperature (>800 °C) treatment under an Ar/H_2 atmosphere, the Fe and Pt molecular precursors are converted to fct FePt nanoparticles without sintering and aggregation. Well-isolated, ~10 nm fct FePt particles were synthesized by this direct method; they have a coercivity of 1100 Oe at 300 K. The coercivity value for FePt-1 (2.6 nm) at 5 K is as high as 11 900 Oe, which is one of the largest values reported for FePt nanoparticles, or any other magnetic nanoparticles. The fct FePt nanoparticles also showed exchange-bias behavior. This simple process opens a new route to the synthesis of well-isolated large fct FePt nanoparticles and can be readily applied to the production of well-separated arrays of fct FePt nanoparticles on a desired substrate for use as magnetic storage media.

METHODS

Synthesis of FePt-1, FePt-2, and FePt-3. Poly(isoprene)-*b*-poly(ethylene oxide) block copolymer (PI-*b*-PEO) was synthesized by anionic polymerization. The M_n value and PEO fraction of PI-*b*-PEO used for the FePt synthesis were found to be 30 000 g mol^{-1} and 0.06, respectively. The molecular weights of PI block and PEO block are 28 800 and 1200 g mol^{-1}, respectively. PI-*b*-PEO has narrow weight distributions with a polydispersity index of 1.13. 3-Glycidoxypropyltrimethoxysilane (GLYMO) and aluminum *sec*-butoxide (molar ratio = 9:1) were hydrolyzed by a two-step acid catalysis to form a sol solution.[7] For the synthesis of FePt-3, 0.15 g of PI-*b*-PEO was dissolved in a mixture of 1.5 mL of THF and 1.5 mL of chloroform. A 31.5 mg portion of dimethylaminomethyl-ferrocene and 41.4 mg of dimethyl(1,5-cyclooctadiene)platinum(II) were dissolved in the block copolymer solution. A 0.9 g portion of organo-aluminosilicate was then added to the polymer−metal precursor solution. Films were cast by evaporation of the solvents on a hot plate at 50 °C and further dried at 130 °C in a vacuum oven for 1 h. The as-synthesized films were heat-treated to 300 °C under Ar/H_2 (5 wt %) and held for 2 h. After cooling to room temperature, the films were heat-treated to 800 °C under Ar/H_2 (5 wt %) and held for

2 h. For the synthesis of FePt-1, 10.5 mg of dimethylaminomethyl-ferrocene and 13.8 mg of dimethyl(1,5-cyclooctadiene)-platinum(II) were dissolved in the block copolymer solution. For the synthesis of FePt-2, 21.0 mg of dimethylaminomethyl-ferrocene and 27.6 mg of dimethyl(1,5-cyclooctadiene)platinum(II) were dissolved in the block copolymer solution. The subsequent steps in the synthetic procedure were the same as those for FePt-3.

Characterization. TEM and HRTEM characterizations were carried out using an EM-2010 microscope (JEOL Ltd.). The XRD study was performed with an X'Pert diffractometer (Cu Kα radiation, PANalytical) with an X'Celerator detector (PANalytical). SAXS data were collected with an apparatus consisting of an 18 kW rotating anode X-ray generator (Cu Kα wavelength = 1.542 Å, Rigaku Co.) and a one-dimensional position-sensitive detector (M. Braun Co.). The Raman spectra were recorded on an FT-Raman spectrometer (Senterra, Bruker Optics). The structure of materials was examined by scanning electron microscopy (FESEM, Hitachi S-4800). We measured magnetizations as functions of temperature and field using a commercial SQUID magnetometer (MPMS 5XL, Quantum Design) from 2 to 350 K. The hysteresis curves were obtained by sweeping the magnetic field between −5 and +5 T.

Acknowledgment. This research was supported by the Basic Science Research Program through the National Research Foundation of Korea (NRF) funded by the Ministry of Education, Science and Technology KRF-2008-313-D00248. This work was further supported by the Midcareer Researcher Program (2009-0084771), through an NRF grant funded by the MEST and by the National Creative Research Initiative Program supported by the National Research Foundation of Korea (NRF). Work at Seoul National University was supported by the National Research Foundation of Korea (Grant Nos. KRF-2008-220-C00012 and R17-2008-033-01000-0). This work was further financially supported by the second stage of the BK 21 program of Korea.

Supporting Information Available: SEM images and TEM images of FePt-2, magnified SEM image and TEM image of FePt-1, TEM image of heat-treated (800 °C) FePt-silica composite materials fabricated using F127, SEM image of FePt (20 wt %)-mesostructured silica/carbon heat-treated at 800 °C under Ar/H_2 (5 wt %), TEM image of a 20 wt % sample and its particle size distribution, particle size distributions obtained from TEM images of FePt-1 and FePt-3, and magnetization curves after zero-field-cooling and field-cooling. This material is available free of charge *via* the Internet at http://pubs.acs.org.

REFERENCES AND NOTES

1. Weller, D.; Moser, A. Thermal Effect Limits in Ultrahigh-Density Magnetic Recording. *IEEE Trans. Magn.* **1999,** *35*, 4423–4439.
2. Peng, D. L.; Hihara, T.; Sumiyama, K. Structure and Magnetic Properties of FePt Alloy Cluster-Assembled Films. *J. Magn. Magn. Mater.* **2004,** *277*, 201–208.
3. Varada, L. C.; Jafelicci, M., Jr. Self-Assembled FePt Nanocrystals with Large Coercivity: Reduction of the fcc-to-$L1_0$ Ordering Temperature. *J. Am. Chem. Soc.* **2006,** *128*, 11062–11066.
4. Sun, S.; Murray, C. B.; Weller, D.; Folks, L.; Moser, A. Monodisperse FePt Nanoparticles and Ferromagnetic FePt Nanocrystal Superlattices. *Science* **2000,** *287*, 1989–1992.
5. Stahl, B.; Gajbhiye, N. S.; Wilde, G.; Kramer, D.; Ellrich, J.; Ghafari, M.; Hahn, H.; Gleiter, H.; Weissmüller, J.; Würschum, R.; *et al.* Electronic and Magnetic Properties of Monodispersed FePt Nanoparticles. *Adv. Mater.* **2002,** *14*, 24–27.
6. Sun, S.; Anders, S.; Thomson, T.; Baglin, J. E. E.; Toney, M. F.; Hamann, H. F.; Murray, C. B.; Terris, B. D. Controlled Synthesis and Assembly of FePt Nanoparticles. *J. Phys. Chem. B* **2003,** *107*, 5419–5425.
7. Rong, C.; Li, D.; Nandwana, V.; Poudyal, N.; Ding, Y.; Wang, Z. L.; Zeng, H.; Liu, J. P. Size-Dependent Chemical and Magnetic Ordering in $L1_0$-FePt Nanoparticles. *Adv. Mater.* **2006,** *18*, 2984–2988.
8. Sun, S. Recent Advances in Chemical Synthesis, Self-Assembly, and Applications of FePt Nanoparticles. *Adv. Mater.* **2006,** *18*, 393–403.
9. Zhao, Z. L.; Chen, J. S.; Ding, J.; Inba, K.; Wang, J. P. The Effect of Additive Ag Layers on the $L1_0$ FePt Phase Transformation. *J. Magn. Magn. Mater.* **2004,** *282*, 105–108.
10. Wang, S.; Kang, S. S.; Nickles, D. E.; Harrell, J. W.; Wu, X. W. Magnetic Properties of Self-Organized $L1_0$ FePtAg Nanoparticle Arrays. *J. Magn. Magn. Mater.* **2003,** *266*, 49–56.
11. Kang, S.; Harrell, J. W.; Nikles, D. E. Reduction of the fcc to $L1_0$ Ordering Temperature for Self-Assembled FePt Nanoparticles Containing Ag. *Nano Lett.* **2002,** *2*, 1033–1036.
12. Lee, D. C.; Mikulec, F. V.; Pelaz, J. M.; Koo, B.; Korgel, B. A. Synthesis and Magnetic Properties of Silica-Coated FePt Nanocrystals. *J. Phys. Chem. B* **2006,** *110*, 11160–11166.
13. Piao, Y.; Kim, J.; Na, H. B.; Kim, D.; Baek., J. S.; Ko, M. K.; Lee, J. H.; Shokouhimehr, M.; Hyeon, T. Wrap−Bake−Peel Process for Nanostructural Transformation from β-FeOOH Nanorods to Biocompatible Iron Oxide Nanocapsules. *Nat. Mater.* **2008,** *7*, 242–247.
14. Kim, J.; Rong, C.; Lee, Y.; Liu, J. P.; Sun, S. From Core/Shell Structured FePt/Fe_3O_4/MgO to Ferromagnetic FePt Nanoparticles. *Chem. Mater.* **2008,** *20*, 7242–7245.
15. Kockrick, E.; Krawiec, P.; Schnelle, W.; Geiger, D.; Schappacher, F. M.; Pöttgen, R.; Kaskel, S. Space-Confined Formation of FePt Nanoparticles in Ordered Mesoporous Silica SBA-15. *Adv. Mater.* **2007,** *19*, 3021–3026.
16. Teng, X.; Yang, H. Synthesis of Face-Centered Tetragonal FePt Nanoparticles and Granular Films from Pt@Fe_2O_3 Core-Shell Nanoparticles. *J. Am. Chem. Soc.* **2003,** *125*, 14559–14563.
17. Chen, M.; Kim, J.; Liu, J. P.; Fan, H.; Sun, S. Synthesis of FePt Nanocubes and Their Oriented Self-Assembly. *J. Am. Chem. Soc.* **2006,** *128*, 7132–7133.
18. Templin, M.; Franck, A.; Chesne, A. D.; Leist, H.; Zhang, Y.; Ulrich, R.; Schadler, V.; Wiesner, U. Organically Modified Aluminosilicate Mesostructures from Block Copolymer Phases. *Science* **1997,** *278*, 1795–1798.
19. Yu, C.; Yu, Y.; Zhao, D. Highly Ordered Large Caged Cubic Mesoporous Silica Structures Templated by Triblock PEO−PBO−PEO Copolymer. *Chem. Commun.* **2000,** 575–576.
20. Garcia, G.; Zhang, Y.; DiSalvo, F.; Wiesner, U. Mesoporous Aluminosilicate Materials with Superparamagnetic g-Fe_2O_3 Particles Embedded in the Walls. *Angew. Chem., Int. Ed.* **2003,** *42*, 1526–1530.
21. Krawitz, A. D. *Introduction to Diffraction in Materials Science and Engineering*; Wiley: New York, 2001; 168.
22. Lee, J.; Orilall, M. C.; Warren, S. C.; Kamperman, M.; DiSalvo, F. J.; Wiesner, U. Direct Access to Thermally Stable and Highly Crystalline Mesoporous Transition-Metal Oxides with Uniform Pores. *Nat. Mater.* **2008,** *7*, 222–228.
23. Warren, S. C.; Messina, L. C.; Slaughter, L. S.; Kamperman, M.; Zhou, Q.; Gruner, S. M.; DiSalvo, F. J.; Wiesner, U. Ordered Mesoporous Materials from Metal Nanoparticle-Block Copolymer Self-Assembly. *Science* **2008,** *320*, 1748–1752.
24. Lettow, J. S.; Han, Y. P.; Schmidt-Winkel, P.; Yang, P.; Zhao, D.; Stucky, G. D.; Ying, J. Hexagonal to Mesocellular Foam Phase Transition in Polymer-Templated Mesoporous Silicas. *Langmuir* **2000,** *16*, 8291–8295.
25. Zhao, D.; Huo, Q.; Feng, J.; Chmelka, B.; Stucky, G. D. Nonionic Triblock and Star Diblock Copolymer and Oligomeric Surfactant Syntheses of Highly Ordered, Hydrothermally Stable, Mesoporous Silica Structures. *J. Am. Chem. Soc.* **1998,** *120*, 6024–6036.
26. Floudas, G.; Ulrich, R.; Wiesner, U. Microphase Separation in Poly(isoprene-b-ethylene oxide) Diblock Copolymer Melts. I. Phase State and Kinetics of the Order-to-Order Transitions. *J. Chem. Phys.* **1999,** *110*, 652–663.
27. Fairclough, J. P. A.; Yu, G.-E.; Mai, S.-M.; Crothers, M.; Mortensen, K.; Ryan, A. J.; Booth, C. First Observation of an Ordered Microphase in Melts of Poly(oxyethylene)-Poly(oxypropylene) Block Copolymers. *Phys. Chem. Chem. Phys.* **2000,** *2*, 1503–1507.

28. Warren, S. C.; DiSalvo, F. J.; Wiesner, U. Nanoparticle-Tuned Assembly and Disassembly of Mesostructured Silica Hybrids. *Nat. Mater.* **2007,** *6*, 156–161.
29. Meiklejohn, W. H.; Bean, C. P. New Magnetic Anisotropy. *Phys. Rev.* **1956,** *102*, 1413–1414.
30. Nogues, J.; Schuller, I. K. Exchange Bias. *J. Magn. Magn. Mater.* **1999,** *192*, 203–232.
31. Skumryev, V.; Stoyanov, S.; Zhang, Y.; Hadjipanayis, G.; Givord, D.; Noguès, J. Beating the Superparamagnetic Limit with Exchange Bias. *Nature* **2003,** *423*, 850–853.
32. Park, J.; An, K.; Hwang, Y.; Park, J.-G.; Noh, H.-J.; Kim, Y. J.; Park, J.-H.; Hwang, N.-M.; Hyeon, T. Ultra-Large-Scale Syntheses of Monodisperse Nanocrylstals. *Nat. Mater.* **2004,** *3*, 891–895.
33. Bae, C. J.; Hwang, Y.; Park, J.; An, K.; Lee, Y.; Lee, J.; Hyeon, T.; Park, J.-G. Inter-Particle and Interfacial Interaction of Magnetic Nano Particles. *J. Magn. Magn. Mater.* **2007,** *310*, e806–e808.